

Neoatherosclerosis assessed with optical coherence tomography in restenotic bare metal and first- and second-generation drug-eluting stents

Lei Song^{1,2,3} · Gary S. Mintz¹ · Dong Yin^{1,2,3} · Myong Hwa Yamamoto^{1,2} · Chee Yang Chin^{1,4} · Mitsuaki Matsumura¹ · Khady Fall² · Ajay J. Kirtane^{1,2} · Manish A. Parikh^{1,2} · Jeffrey W. Moses^{1,2} · Ziad A. Ali^{1,2} · Richard A. Shlofmitz⁵ · Akiko Maehara^{1,2}

Received: 20 October 2016 / Accepted: 1 March 2017 / Published online: 9 March 2017
© Springer Science+Business Media Dordrecht 2017

Abstract Although reported in bare metal stents (BMS) and first-generation drug-eluting stents (DES), little is known about neoatherosclerosis in second-generation DES. We used optical coherence tomography to evaluate neoatherosclerosis among different stent generations. Overall, 274 in-stent restenosis (ISR) lesions (duration from implantation 56.9 ± 47.2 months) in 274 patients were assessed for the presence of neoatherosclerosis. Neoatherosclerosis was identified in 38.7% of lesions (106/274): 23.0% second-generation DES (38/165), 65.1% first-generation DES (54/83), and 53.8% BMS (14/26). In the neoatherosclerosis cohort ($n=106$), more stent underexpansion or fracture/deformation was observed in second-generation DES, whereas thrombus, without plaque rupture, or evagination was more common in first-generation DES. In multivariable analyses, duration from implantation >1 year (OR: 2.44, 95% CI 1.12–5.31; $p=0.03$), absence of angiotensin-converting enzyme inhibitors/angiotensin II receptor blockers (OR 1.95, 95% CI 1.10–3.44; $p=0.02$) or statins at the time of ISR (OR 3.12, 95% CI 1.42–6.84; $p=0.01$), and

first-generation vs first-generation DES (OR 5.32, 95% CI 2.82–10.10; $p<0.001$) correlated with a higher prevalence of neoatherosclerosis. Duration from implantation <1 year (OR 2.17, 95% CI 1.03–4.55; $p=0.04$) and thin fibrous cap, thrombus, or rupture (OR 2.72, 95% CI 1.15–6.39; $p=0.02$) were independent predictors for acute coronary syndromes presentation. Neoatherosclerosis is an important ISR mechanism, especially in first generation DES.

Keywords Imaging · Optical coherence tomography · In-stent restenosis · Drug-eluting stent · Bare metal stent

Introduction

Drug-eluting stents (DES) have significantly reduced in-stent restenosis (ISR) and the need for revascularization compared with bare metal stents (BMS) [1, 2]. Although historically considered a stable condition, recent studies have shown that acute coronary syndromes (ACS) can account for 20–70% of ISR presentations, depending on patient population, lesion characteristics, and stent type [3]. The primary explanation for ACS ISR presentation has been the development of in-stent neoatherosclerosis [4]; however, most reports of neoatherosclerosis have been based on BMS and first-generation DES [4, 5]. The aim of this study was to use optical coherence tomography (OCT), the technique of choice to assess neoatherosclerosis, to investigate the prevalence and patterns of in-stent neoatherosclerosis among second-generation DES as compared to BMS and first-generation DES.

Electronic supplementary material The online version of this article (doi:10.1007/s10554-017-1106-2) contains supplementary material, which is available to authorized users.

✉ Akiko Maehara
amaehara@crf.org

¹ Cardiovascular Research Foundation, 1700 Broadway, 9th Floor, New York, NY 10019, USA

² New York-Presbyterian Hospital/Columbia University Medical Center, New York, NY, USA

³ Nation Center for Cardiovascular Disease, China Peking Union Medical College, Fuwai Hospital, Beijing, China

⁴ National Heart Centre Singapore, Singapore, Singapore

⁵ St. Francis Hospital, Roslyn, NY, USA

Materials and methods

We retrospectively reviewed 483 patients (505 stented lesions) who underwent OCT follow-up at 2 sites in the United States (New York-Presbyterian Hospital, New York, New York; St. Francis Hospital, Roslyn, New York) from February 2011 to January 2016. ISR was an in-stent minimum lumen area (MLA) $<3.0 \text{ mm}^2$ detected by OCT [6, 7]. We excluded 189 with an MLA $\geq 3.0 \text{ mm}^2$; 6 with stent thrombosis, but not ISR; 19 with poor image quality; 14 with multiple ISR lesions (only the most severe ISR was included); and 3 saphenous vein graft ISR lesions.

Stents were divided into 3 groups: BMS; first-generation DES [Cypher (Cordis Corp, Miami Lakes, Florida) sirolimus-eluting stent (SES) and TAXUS (Boston Scientific, Natick, Massachusetts) paclitaxel-eluting stent (PES)]; and second-generation DES [Promus (Boston Scientific) everolimus-eluting stent (EES), XIENCE (Abbott Vascular, Santa Clara, California) EES, Endeavor (Medtronic, Santa Rosa, California) and Resolute (Medtronic) zotarolimus-eluting stent (ZES)]. For those stents in which the specific stent type was not identifiable, we based the differentiation of BMS vs first-generation DES vs second-generation DES on the dates of FDA approval and dates of first- and second-generation DES availability at our two hospitals. Specifically, if the implantation date was between June 2004 and June 2008, we consider this as first-generation DES; if the implantation date was after January 2009, we consider this as second-generation DES. The Cypher stent was approved on April 24, 2003, Endeavor stent on February 1, 2008, and Xience and Promus stents on July 1, 2008.

Clinical presentation was divided into ACS (unstable angina [no ST-segment elevation and no biomarker release, but angina at rest, new-onset angina, or crescendo anginal pattern], ST-segment elevation myocardial infarction (MI), or non-ST-segment elevation MI [no ST-segment elevation with biomarker release]) versus non-ACS.

Ostial lesions began $<3 \text{ mm}$ of the origin of a major epicardial artery. A bifurcation lesion had a sidebranch diameter $>1.5 \text{ mm}$ [8].

An OCT catheter (C7 Dragonfly or Dragonfly Duo, St Jude Medical, St. Paul, Minnesota) was introduced distal to the lesion; contrast media was injected via the guiding catheter at a rate of 4–5 mL/s during pullback and image acquisition. OCT images were acquired using frequency-domain OCT (C7XR, ILUMIEN, or ILUMIEN OPTIS OCT Imaging Systems, St Jude Medical) at a pullback speed of 5 or 10 frame/mm and slice interval of 0.2 mm or 0.1 mm, respectively [9]. Off-line analysis was done by agreement of 2 independent cardiologists (LS and AM) blinded to clinical and angiographic characteristics and using proprietary software (St. Jude Medical) after confirming calibration.

Cross-sectional OCT images were evaluated for all slices, and stent and intra-stent lumen cross-sectional areas (CSA) were measured at the MLA, minimum stent area (MSA), and maximum neointimal hyperplasia (NIH) sites [10]. Stent CSA was measured by joining middle points of the strut blooming. If the stent was covered by high signal attenuation tissue, stent CSA was delineated by comparing proximal or distal slices. Percentage of NIH was calculated as $[(\text{stent} - \text{lumen})/\text{stent}] \times 100$. Restenotic length was classified as focal ($<10 \text{ mm}$), multifocal, or diffuse ($>10 \text{ mm}$) [11]. Proximal and distal reference lumen areas were the largest lumen CSA within 5 mm proximal and distal to stent edges, but before significant sidebranches ($>1.5 \text{ mm}$ in diameter).

Neoatherosclerosis was NIH that was lipidic or contained neo-calcification/calcified nodule or neointimal rupture [5]. The distribution of neoatherosclerosis was categorized as (1) focal ($<10 \text{ mm}$ in length); (2) multifocal ($<10 \text{ mm}$ in length and $>5 \text{ mm}$ apart); or (3) diffuse ($\geq 10 \text{ mm}$ in length). Lipidic NIH contained signal-poor regions with diffuse borders in at least 3 connected frames; thin-cap fibroatheroma (TCFA) had lipidic NIH with a fibrous cap thickness $\leq 65 \mu\text{m}$ (Fig. 1a) [12]. Foamy macrophage accumulation (Fig. 1b) contained high-intensity, signal-rich, linear regions with sharp attenuation and narrow trailing shadows that changed frame-by-frame. Neointimal calcium was a signal-poor area with a well-delineated border (Fig. 1c) [12]; protrusion of calcium through stent struts was not evidence of neoatherosclerosis. A calcified nodule had fibrous cap disruption over protruding nodular calcification superimposed on a calcified plate with superficial thrombus (Fig. 1d). In the absence of a calcified nodule or a strut within the calcium (confirmed by checking proximal and distal frames), calcium was considered to represent protrusion of native lesion calcium through the struts (Fig. 1e). Thrombus with or without neointimal rupture was identified as previously reported (Fig. 1f, g) [13]. Layered NIH was a homogeneous surface underlying lipidic or homogeneous plaque having a different OCT intensity compared to the surface layer (Fig. 1h). In addition, the presence of cholesterol crystals, microvessels (Fig. 1i), and peri-strut low intensity area (Fig. 1j) were noted [14].

A malapposed strut had a measured distance between its surface and the adjacent lumen border greater than the strut thickness (BMS) or greater than the sum of the thickness of the strut plus polymer (SES $\geq 160 \mu\text{m}$, PES $\geq 130 \mu\text{m}$, ZES $\geq 110 \mu\text{m}$, and EES $\geq 100 \mu\text{m}$). Malapposition distance was measured from the middle of the strut blooming to the adjacent lumen border [13, 14]. Evagination was outward protrusion of the luminal contour between well-apposed struts with a maximum protrusion depth $>10\%$ of the mean stent diameter within the same frame (Fig. 1k) [15]. Stent fracture was separation of the stent into 2 pieces divided by

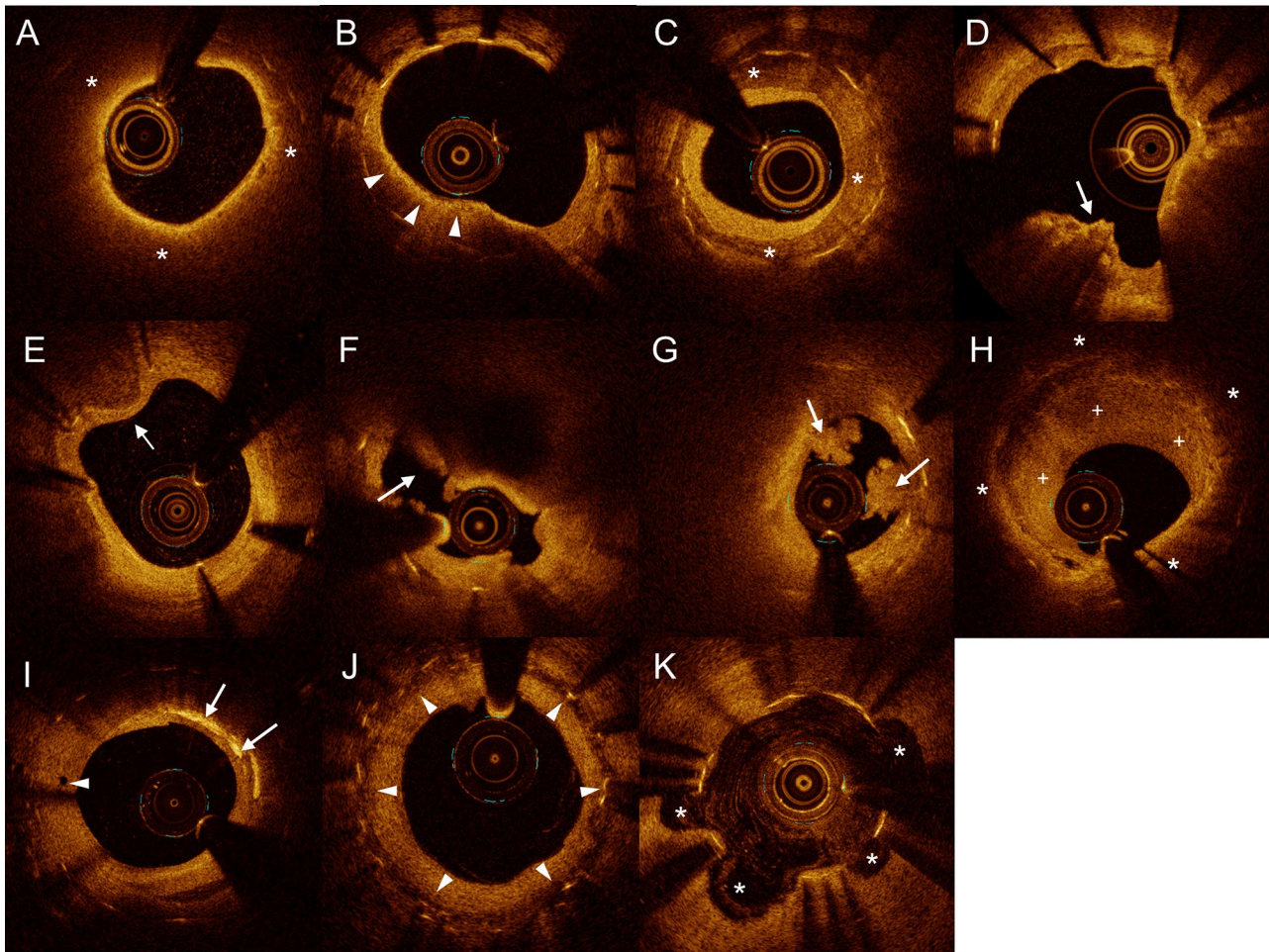


Fig. 1 Examples of Neoatherosclerosis. **a** Lipidic neointima (asterisks); **b** foamy macrophages (arrowheads); **c** calcified neointima (asterisks); **d** calcified nodule (arrow); **e** native calcium protrusion through the stent strut (arrow); **f** lipidic neointima with rupture and thrombus (arrow); **g** lipidic neointima with thrombus (arrow) without

rupture; **h** multiple layer neoatherosclerosis, top layer (+) and bottom layer (asterisks); **i** cholesterol crystals (arrows) with a microvessel (arrowhead); **j** peri-strut low-intensity area (arrowheads); **k** evaginations (asterisks)

image slices with $\geq 120^\circ$ of the stent circumference having no visible struts. Stent deformation was distortion, shortening, or severe maldistribution of struts [16].

Only 1 ISR lesion was analyzed per patient. Non-normally distributed continuous variables were reported as median with first and third quartiles and compared with the Wilcoxon rank sum test; normally distributed continuous variables were reported as mean and standard deviation and compared with analysis of variance. Categorical variables were summarized as numbers (percentages) and compared using χ^2 statistics or Fisher exact test, as appropriate. Post-hoc analyses for multiple comparisons were done using Bonferroni corrections for categorical variables or least significant difference for continuous variables. Bivariate correlation was performed using the Pearson correlation coefficient. A multivariable logistic model was performed to identify factors associated with ACS as the ISR

clinical presentation or in-stent neoatherosclerosis; clinically important variables as well as variables statistically significant on univariate analysis covariates were entered into the model.

P-value < 0.05 was considered significant. All statistical analyses were performed using SPSS software version 22.0 (IBM, Armonk, New York).

Results

Among 274 evaluable ISR lesions, 196 (71.5%) had acute coronary syndrome as the clinical presentation. Among other patients, 35 presented with stable angina (12.8%); 37 were without ischemia symptoms, but had a positive stress test or $\text{FFR} < 0.8$ (13.5%); and only 6 (2.2%) had no ischemia evidence and did not have an intervention.

Neoatherosclerosis was identified in 38.7% of lesions (106/274): 23.0% of second-generation DES (38/165), 65.1% first-generation DES (54/83), and 53.8% of BMS (14/26).

Patient and angiographic characteristics have been shown in Table 1 (BMS vs first-generation DES vs second-generation DES) and supplemental Table 1 (neoatherosclerosis vs no neoatherosclerosis). When we compared patients with neoatherosclerosis to those without neoatherosclerosis (supplemental Table 1); (1) duration from stent implantation was longer; (2) there was less frequent usage of statins, ADP agonists, or ACE inhibitors or angiotensin II receptor blockers; and (3) ostial lesion location

was less common. There was no significant difference in risk factors, clinical presentation or angiographic location, and appearance in patients with neoatherosclerosis among BMS, first-generation DES, or second-generation DES (Table 1).

In OCT-detected ISR with neoatherosclerosis, the MSA was smaller in DES (second-generation DES 4.62 ± 1.76 mm², first-generation DES 4.88 ± 1.52 mm²) compared with BMS (6.32 ± 1.39 mm², $p=0.003$), as was the stent area at the MLA or the maximum NIH sites (Table 2).

The distribution of neoatherosclerosis was more focal in second generation DES vs others ($p=0.04$). Of note, neoatherosclerosis always clustered within 0.5 mm of the MLA

Table 1 Clinical and angiographic characteristics in patients with neoatherosclerosis

Variable	Second-generation DES (n=38)	First-generation DES (n=54)	BMS (n=14)	p-value
Age (years)	68.3 ± 12.9	66.4 ± 10.0	66.9 ± 10.8	0.73
Female	12 (31.6%)	15 (27.8%)	3 (21.4%)	0.76
Duration from implantation (months)	32 ± 21	101 ± 19	152 ± 49	<0.001*
>1 year	29 (76.3%)	54 (100%)	14 (100%)	<0.001
>5 years	5 (13.2%)	53 (98.1%)	12 (85.7%)	<0.001
Diabetes mellitus	19 (50.0%)	20 (37.0%)	6 (42.9%)	0.46
Hypertension	32 (84.2%)	43 (79.6%)	11 (78.6%)	0.83
Hyperlipidemia	31 (81.6%)	40 (74.1%)	12 (85.7%)	0.52
Current smoker (<1 month)	3 (7.9%)	6 (11.1%)	1 (7.1%)	0.83
Renal insufficiency [†]	4 (10.5%)	7 (13.0%)	3 (21.4%)	0.62
Prior myocardial infarction	12 (31.6%)	17 (31.5%)	5 (35.7%)	0.95
Prior coronary artery bypass grafting	7 (18.4%)	8 (14.8%)	3 (21.4%)	0.81
Presentation with acute coronary syndromes	32 (84.2%)	39 (72.2%)	11 (78.6%)	0.39
Medication at the time of in-stent restenosis				
Statin	29 (76.3%)	38 (70.4%)	13 (92.9%)	0.16
Aspirin	32 (84.2%)	45 (83.3%)	11 (78.6%)	0.89
ADP antagonist	31 (81.6%)	34 (63.0%)	6 (42.9%)	0.02 [‡]
ACE inhibitor/ARB	20 (52.6%)	21 (38.9%)	6 (42.9%)	0.42
Vessel				
Left anterior descending	18 (47.4%)	32 (59.3%)	10 (71.4%)	0.26
Left circumflex	9 (23.7%)	8 (14.8%)	2 (14.3%)	0.52
Right	11 (28.9%)	14 (25.9%)	2 (14.3%)	0.53
Lesion characteristics				
Bifurcation	10 (26.3%)	15 (27.8%)	3 (21.4%)	0.89
Ostial location	3 (7.9%)	3 (5.6%)	2 (14.3%)	0.58
ISR ≥ 2 times	16 (42.1%)	14 (25.9%)	5 (35.7%)	0.26
ISR at overlapped stents	10 (26.3%)	11 (20.4%)	4 (28.6%)	0.72
ISR at gap between stents	1 (2.6%)	2 (3.7%)	0 (0%)	0.62

Values are n (%) or mean ± standard deviation

ACE angiotensin-converting enzyme; ADP adenosine diphosphate; ARB angiotensin II receptor blocker; BMS bare metal stent; DES drug-eluting stent

*P-value driven by second-generation vs first-generation DES, $p<0.001$; second-generation DES vs bare metal stent, $p<0.001$; first-generation DES vs bare metal stent, $p=0.03$

[†]Creatinine clearance <60 mL/min as calculated by the Cockcroft–Gault equation

[‡]Second-generation DES vs BMS, $p=0.04$

Table 2 Optical coherence tomography quantitative findings in neoatherosclerosis

Variable	Second-generation DES (n=38)	First-generation DES (n=54)	BMS (n=14)	p-value
Minimum lumen site				
Minimum lumen area (mm ²)	1.83±0.67	1.83±0.64	2.08±0.66	0.40
Stent area (mm ²)	5.39±2.15	5.58±1.67	7.03±1.85	0.02*
NIH (%)	61.6±17.8	64.9±14.7	68.7±13.8	0.32
Minimum stent area site				
Same as minimum lumen area site	18 (47.4%)	25 (46.3%)	7 (50.0%)	0.97
Minimum stent area (mm ²)	4.59±1.69	4.88±1.59	6.32±1.39	0.003 [†]
Minimum stent area <4.0 mm ²	16 (42.1%)	20 (37.0%)	1 (7.1%)	0.03 [‡]
Maximum NIH site				
Same as minimum lumen site	33 (86.8%)	43 (79.6%)	10 (71.4%)	0.42
Stent area (mm ²)	5.58±2.08	5.70±1.51	7.39±1.56	0.003 [§]
Maximum NIH (%)	62.3±17.5	64.4±14.5	71.0±9.7	0.20
Maximum NIH >50%	27 (71.1%)	47 (87.0%)	13 (92.9%)	0.08
Proximal reference lumen area (mm ²)	7.80±2.17	7.21±2.02	7.11±2.27	0.54
Distal reference lumen area (mm ²)	5.32±1.61	4.87±1.64	5.57±1.58	0.37
ISR length				
Diffuse (≥10 mm)	15 (39.5%)	20 (37.0%)	3 (21.4%)	0.47
Focal (<10 mm)	16 (42.1%)	18 (33.3%)	8 (57.1%)	0.25
Multi-focal	7 (18.4%)	16 (29.6%)	3 (21.4%)	0.45
ISR at stent edge	6 (15.8%)	12 (22.2%)	3 (21.4%)	0.73

Values are n (%), mean ± standard deviation, or median (interquartile range)

BMS bare metal stent; DES drug-eluting stent; ISR in-stent restenosis; NIH neointimal hyperplasia

*P-value driven by second-generation DES vs BMS, p=0.006, first-generation DES vs BMS, p=0.01

[†]Second-generation DES vs BMS, p=0.001, first-generation DES vs BMS, p=0.003

[‡]Second-generation DES vs BMS, p=0.045, first-generation DES vs BMS=0.08

[§]Second-generation DES vs BMS, p=0.001, first-generation DES vs BMS, p=0.002

site (Table 3). Based on measurements at the MLA site, ISR with neoatherosclerosis was divided into dominant underexpansion (MSA <4.0 mm², NIH ≤50%), dominant NIH (MSA ≥4.0 mm² and NIH >50%), and mixed underexpansion and NIH (MSA <4.0 mm² and NIH >50%). There was a trend for more underexpansion in second-generation DES with neoatherosclerosis (Fig. 2).

Despite the difference in duration from implantation, lipidic NIH, calcified NIH, and foamy macrophages were similar among the 3 types of stents; and the maximum lipid angle had no correlation with duration since implantation. Restenotic second-generation DES with neoatherosclerosis had a smaller maximum angle of neointimal calcium, but a higher frequency of native calcified tissue protruding through stent struts. Cholesterol crystals were observed in 16.0% of ISR with neoatherosclerosis (Table 3) –13.8% in lipidic NIH or rupture (9 out of 65) and 15.9% in calcified NIH (10 out of 63). When we compared SES vs PES, SES had more TCFA (62.5% vs 28.6%, p=0.04) and thrombus (56.2% vs 19.0%, p=0.02); but no other differences were found. When we compared EES vs ZES, there were no significant differences.

The maximum angle of neointimal calcium was positively correlated with the maximum angle of calcium behind the stent (r=0.74, p<0.001); and this correlation was observed in BMS, first-generation DES, and second-generation DES (Fig. 3). Also, there was a weak correlation between the maximum angle of neointimal calcium and the duration from implantation (r=0.47, p<0.001) (Fig. 3). Stent fracture/deformation was more common in second-generation DES with neoatherosclerosis while thrombus without rupture plaque, or evagination were more common in first-generation DES (Tables 3, 4). Overall, 71.4% (5/7) of stent fractures/deformation, but only 16.7% (3/18) of malappositions and 9.5% (2/21) of evaginations were located at the MLA site (Table 4).

In multivariable logistic regression models, duration from implantation >1 year (odds ratio [OR] 2.44, 95% confidence interval [CI] 1.12–5.31; p=0.03), absence of angiotensin-converting enzyme (ACE) inhibitors/angiotensin II receptor blockers (ARB) (OR 1.95, 95% CI 1.10–3.44; p=0.02) or statin use (OR 3.12, 95% CI 1.42–6.84; p=0.01), and first-generation vs second-generation DES (OR 5.32, 95% CI 2.82–10.10; p<0.001) correlated

Table 3 Optical coherence tomography qualitative findings in neoatherosclerosis

Variable	Second-generation DES (n=38)	First-generation DES (n=54)	BMS (n=14)	p-value
Duration from implantation (months)	32 ± 21	101 ± 19	152 ± 49	<0.001*
Macrophage	31 (81.6%)	50 (92.6%)	13 (92.9%)	0.24
Maximum angle (°)	153 (112–228)	174 (143–290)	142 (127–176)	0.19
Neoatherosclerosis distribution as focal	28 (73.7%)	27 (50.0%)	6 (42.9%)	0.04
Lipidic NIH	24 (63.2%)	31 (57.4%)	10 (71.4%)	0.60
Maximum angle (°)	165 (124–199)	197 (138–287)	141 (134–161)	0.09
Thin-cap fibroatheroma	11 (28.9%)	21 (38.9%)	4 (28.6%)	0.55
Neointimal rupture	1 (2.6%)	7 (13.0%)	3 (21.4%)	0.07
Thrombus	4 (10.5%)	18 (33.3%)	1 (7.1%)	0.01 [†]
Maximum area (mm ²)	0.08 (0.05–0.18)	0.33 (0.06–0.75)	0.18	0.34
Without rupture	3 (7.9%)	13 (24.1%)	0 (0%)	0.01
Layered NIH	8 (21.1%)	3 (5.6%)	2 (14.3%)	0.07
Calcified NIH	21 (55.3%)	34 (63.0%)	8 (57.1%)	0.75
Maximum angle (°)	77 (65–121)	139 (92–220)	196 (88–335)	0.01 [‡]
Calcium with attenuation	11 (28.9%)	26 (48.1%)	6 (42.9%)	0.18
Calcified nodule	2 (5.3%)	4 (7.4%)	0 (0%)	0.38
Native calcium protrusion through struts	6 (15.8%)	5 (9.3%)	0 (0%)	0.12
Calcium behind stent	30 (78.9%)	43 (79.6%)	11 (78.6%)	1.00
Maximum angle (°)	165 (96–269)	157 (110–281)	137 (95–276)	0.87
Cholesterol crystal	5 (13.2%)	10 (18.5%)	2 (14.3%)	0.77
Microvessel	14 (36.8%)	12 (22.2%)	9 (64.3%)	0.01 [§]
Peri-strut low-intensity area	20 (52.6%)	22 (40.7%)	11 (78.6%)	0.04
Located at stent edge	19 (50.0%)	16 (29.6%)	10 (71.4%)	0.01

Values are n (%) or median (interquartile range)

BMS bare metal stent; DES drug-eluting stent; NIH neointimal hyperplasia

*P-value driven by second-generation vs first-generation DES, $p < 0.001$; second-generation DES vs bare metal stent, $p < 0.001$; first-generation DES vs bare metal stent, $p = 0.03$

[†]Second-generation DES vs first-generation DES, $p = 0.03$

[‡]Second-generation DES vs first-generation DES, $p = 0.04$, second-generation DES vs BMS, $p = 0.04$

[§]First-generation DES vs BMS, $p = 0.01$

^{||}First-generation DES vs BMS, $p = 0.04$

with a higher prevalence of neoatherosclerosis. Duration from implantation <1 year (OR 2.17, 95% CI 1.03–4.55; $p = 0.04$) and TCFA, thrombus, or rupture within the NIH (OR 2.72, 95% CI 1.15–6.39; $p = 0.02$) were independent predictors for ACS presentation (Table 5).

Discussion

The principal findings of the present study were the following. (i) Neoatherosclerosis was a frequent finding in restenotic DES and BMS lesions. (ii) The prevalence or amount of lipidic or calcified NIH was similar among stent types. (iii) Thrombus, without ruptured plaque, or evagination was observed more commonly in first-generation DES, but stent underexpansion or stent fracture/deformation was observed more commonly in second-generation DES. (iv)

Duration from implantation >1 year, absence of ACE inhibitors/ARBs or statins, and first-generation (versus second-generation) DES were associated with higher prevalence of neoatherosclerosis.

In the present study, there was a significant difference in the rate of neoatherosclerosis among 3 groups and the second-generation DES was associated with a lower prevalence of neoatherosclerosis after adjustments. Though there was a different duration from implantation to OCT follow-up among the 3 ISR groups, the earliest case showing neoatherosclerotic changes was 3 months for second-generation DES, 19 months for first-generation DES, and 27 months for BMS. Using OCT, Kang et al. reported 50 restenotic first-generation DES and found neoatherosclerosis in 90% of the lesions at a median of 32.2 months [4]. On the contrary, most BMS neoatherosclerosis occurred much later as also reported by Yonetsu et al. in a similar

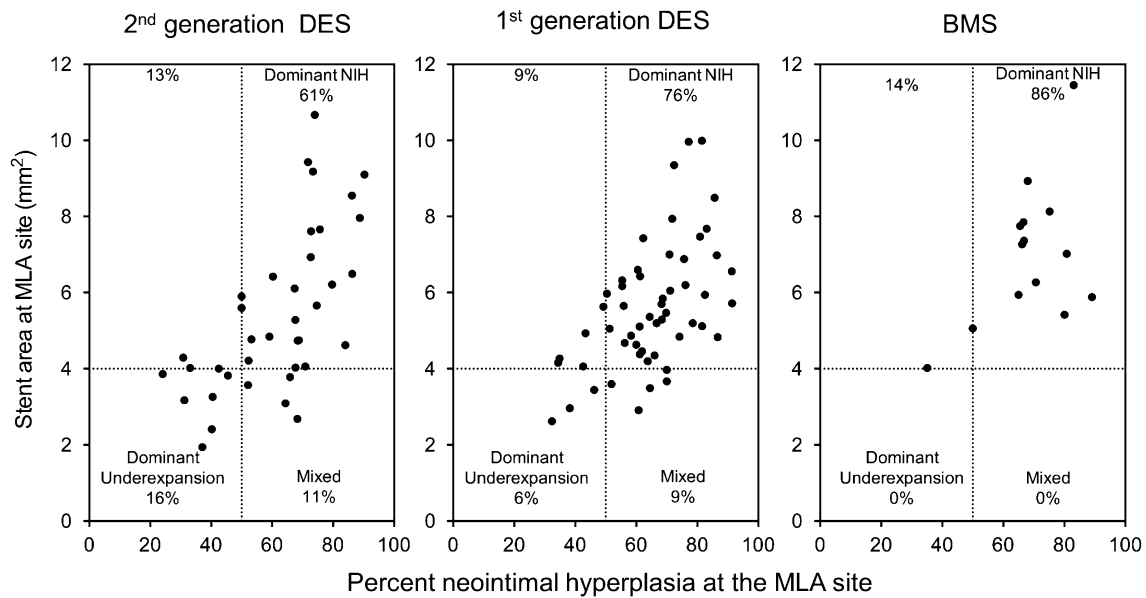


Fig. 2 Percent Neointimal Hyperplasia and Stent Area at the Minimum Lumen Site Among Different Stents In-stent restenosis lesions with neoatherosclerosis were divided into dominant underexpansion (MSA < 4.0 mm², NIH ≤ 50%) dominant NIH (MSA ≥ 4.0 mm² and

NIH > 50%), and mixed underexpansion and NIH (MSA < 4.0 mm² and NIH > 50%), based on the measurements at the minimum lumen area site. minimum stent area (MSA); neointimal hyperplasia (NIH)

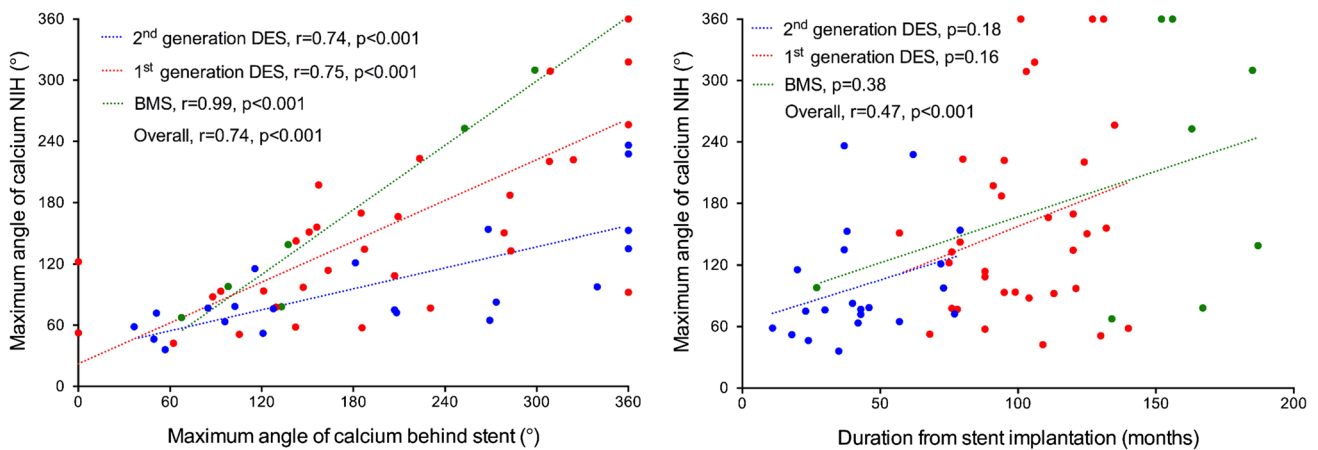


Fig. 3 Correlation Between Maximum Angle of Calcified Neointima vs Calcium Behind Stents and Duration From Implantation (*left*) Overall, the maximum angle of calcium in NIH was positively correlated with the maximum angle of calcium behind the stent struts (r = 0.74, p < 0.001) and this correlation was observed in each BMS,

first-generation DES, or second-generation DES was also correlated with the maximum angle of calcium in NIH; (*right*) the maximum angle of calcium in NIH was positively correlated with the duration from implantation (r = 0.47, p < 0.001). neointimal hyperplasia (NIH)

retrospective OCT study in which the presence of neoatherosclerosis in DES was greater than in BMS ≤ 48 months, but there was no difference > 48 months [17]. The histopathological study by Nakazawa et al. also demonstrated that > 40% of DES showed atherosclerotic changes by 9 months after stenting, but that BMS rarely developed neoatherosclerosis until 4 years [5]. Using angiography, the proportion of BMS with yellow neointima increased from 4% at 6–12 months to 58% at 4 years [18]. Second-generation

DES (EES) was reported to have a similar frequency of neoatherosclerosis (29%) versus first-generation DES (35% for SES, 19% for PES) [19]. However, a more recent study including 212 DES demonstrated that second-generation DES had less neoatherosclerosis (10.8% vs. 45.5%) with a shorter duration from implantation (12.4 months vs. 55.4 months) compared with first-generation DES [20].

Mechanisms underlying increased and earlier neoatherosclerosis in DES are considered multifactorial. In our study

Table 4 Optical coherence tomography mechanical findings in neoatherosclerosis

Variable	Second-generation des (n=38)	First-generation DES (n=54)	BMS (n=14)	p-value
Stent fracture/deformation	5 (13.2%)	1 (1.9%)	1 (7.1%)	0.09
Located at the minimum lumen site	4 (10.5%)	1 (1.9%)	0 (0%)	0.09
Stent fracture	5 (13.2%)	0 (0%)	1 (7.1%)	0.01*
Deformation	2 (5.3%)	1 (1.9%)	0 (0%)	0.43
Strut malapposition	7 (18.4%)	11 (20.4%)	0 (0%)	0.06
Located at minimum lumen site	2 (5.3%)	1 (1.9%)	0 (0%)	0.43
Located at stent edge	2 (5.3%)	7 (13.0%)	0 (0%)	0.12
Calcium behind malapposition	4 (10.5%)	8 (14.8%)	0 (0%)	0.14
Multifocal	6 (15.8%)	6 (11.1%)	0 (0%)	0.13
Maximum malapposition angle (°)	360 (266–360)	180 (103–288)	–	0.06
Maximum malapposition depth (mm)	0.31 (0.20–0.66)	0.36 (0.25–0.41)	–	0.68
Evagination	7 (18.4%)	14 (25.9%)	0 (0%)	0.03 [†]
Located at minimum lumen site	1 (2.6%)	1 (1.9%)	0 (0%)	0.73
Located at stent edge	5 (13.2%)	10 (18.5%)	0 (0%)	0.08
Multi-focal	2 (5.3%)	5 (9.3%)	0 (0%)	0.28
Maximum area (mm ²)	0.17 (0.16–0.33)	0.19 (0.13–0.31)	–	0.43
Maximum depth (mm)	0.31 (0.28–0.38)	0.31 (0.25–0.36)	–	0.55

Values are n (%) or median (interquartile range)

BMS bare metal stent; DES drug-eluting stent

*P-value driven by second-generation DES vs first-generation DES, p=0.03

[†]first-generation DES vs BMS, p=0.08

Table 5 Multivariable logistic regression analyses

Variable	Yes	No	Odds ratio (95% confidence interval)	p-value
In-stent neoatherosclerosis, n	106	168		
Duration from implantation >1 year	95 (89.6%)	115 (68.5%)	2.44 (1.12–5.31)	0.03
Absence of ACE inhibitors/ARB	59 (55.7%)	68 (40.5%)	1.95 (1.10–3.44)	0.02
Absence of Statin	26 (24.5%)	17 (10.1%)	3.12 (1.42–6.84)	0.01
Type of stent				
First-generation (vs. second-generation) DES	54 (50.9%)	29 (17.3%)	5.32 (2.82–10.10)	<0.001
BMS (vs. second-generation DES)	14 (13.2%)	12 (7.1%)	5.21 (2.10–12.99)	<0.001
ACS as in-stent restenosis presentation, n	196	78		
Duration from implantation <1 year	52 (26.5%)	12 (15.4%)	2.17 (1.03–4.55)	0.04
TCFA, thrombus, or rupture	52 (26.5%)	10 (12.8%)	2.72 (1.15–6.39)	0.02

Values are n (%) unless otherwise indicated

ACE angiotensin-converting enzyme; ACS acute coronary syndrome; ARB angiotensin II receptor blockers; TCFA thin-cap fibroatheroma

DES (especially first-generation DES) appeared to have more malapposition, evagination, and thrombus without rupture indicating a worse vessel reaction. A study using thrombus aspirates showed that very late stent thrombosis correlated with vessel remodeling and histopathological signs of vascular inflammation [21]. An OCT study by Radu et al. demonstrated that SES had a significantly higher prevalence of evaginations (27%) during 5 years of follow-up compared with second-generation DES (2% for

ZES, 3% for EES) with a shorter 1 year follow-up that was associated with long-term stent uncoverage, malapposition, and thrombosis [15].

Although NIH was the dominant pattern in all 3 ISR groups, neoatherosclerosis occurred in ISR lesions with dominant underexpansion, particularly second-generation DES. Neoatherosclerosis superimposed on a smaller MSA in second generation stents may have contributed to the clinical presentation and its time-course. Seven of the

restenotic stents with neoatherosclerosis in the current study also had evidence of strut fracture. Previous studies reported a higher prevalence of stent fracture in first-generation DES (0.8–8.4%) [22] versus second-generation DES (1.7–2.9%) [23]. Kang et al. reported the coexistence of neoatherosclerosis and stent fracture, but in the setting of stent thrombosis [24].

In a pathology study by Nakazawa et al., younger patient age, longer duration since implantation, first-generation DES (versus BMS), and underlying unstable plaques were independent predictors for neoatherosclerosis [5]. Yonetsu et al. identified that longer implant duration (≥ 48 months), first-generation DES, current smoking, chronic kidney disease, and absence of ACE inhibitor/ARB use were determinants of OCT-detected neoatherosclerosis [17]. A more recent OCT study by Lee et al. reported that chronic kidney disease, low-density lipoprotein cholesterol >70 mg/dL, and stent age, but not DES type were independent predictors for neoatherosclerosis [20]. Stent age has been the strongest and most consistent factor predicting neoatherosclerosis [5, 17, 20], and lipid-laden neointima or TCFA increased with time in both BMS and DES [4]. In general, our current study was consistent with the findings from these previous publications.

Calcification within the NIH was the dominant pattern of neoatherosclerosis in the current cohort. A previous histopathological study showed that fragmented or sheet-like calcium derived from collagen, extracellular matrix, or smooth muscle cells was a unique manifestation in neoatherosclerosis, different from the microcalcification pattern in native plaque [25]. Calcified NIH was associated with severe calcification behind stent struts as well as older stent age consistent with a previous study showing that in-stent neoatherosclerosis was closely associated with progression of native coronary atherosclerosis [26]. Notably, we identified 6 cases of calcified nodules inside the neointima—one of the less common, but characteristic manifestations of neoatherosclerosis [27]. A calcified nodule could be one possible cause of a thrombotic event in neoatherosclerosis, similar to what has been seen in native lesions.

In the current study ACS, mostly unstable angina, was the presentation in three-quarters of the patients [28]. Although we found that thrombus as a trigger of ACS was more common in first-generation DES (mostly white thrombi that were relatively small), the presentation of ACS was irrespective of stent type.

This was a retrospective observational study; the indications for follow-up OCT varied among the patients. Second, there was a difference in the duration from implantation among the three stent groups. Third, because the present study was not designed as a serial analysis (no index images), the results did not assess the natural history of the neointima, including neointimal calcium. We only assessed

ISR with neoatherosclerosis to decrease the selection bias as much as possible. The data on the rate of neoatherosclerosis development between first- and second-generation DES should be interpreted with caution since first-generation DES have been available for 5+ years longer than second-generation DES. Fourth, because of the limited sample size and some difficulties identifying specific types of first- or second-generation DES, we could not demonstrate distinctive properties among different types of DES especially second-generation DES. Fifth, there was limited information regarding the original stent implantation procedure. Finally, the criteria for OCT-determined neoatherosclerosis still lack absolute consensus, with a discrepancy between OCT and histopathological findings. Thus, we may have over- or underestimated the presence of neoatherosclerosis.

Acknowledgements The authors thank Dominic P. Francese, MPH, for assistance in preparing the manuscript.

Compliance with ethical standards

Conflict of interest Lei Song: Research Grant—Boston Scientific. Gary S. Mintz: Consultant—Boston Scientific, ACIST; fellowship/grant support—Volcano, Boston Scientific, InfraRedx; honoraria—Boston Scientific, ACIST. Dong Yin: Research Grant—Boston Scientific. Chee Yang Chin: Honoraria—ACIST. Ajay J. Kirtane: Institutional research grants to Columbia University from Boston Scientific, Medtronic, Abbott Vascular, Abiomed, St. Jude Medical, and Eli Lilly. Manish A. Parikh: Speakers bureau—Abbott Vascular, Boston Scientific, Medtronic, CSI, Corindus; advisory board—Abbott Vascular, Medtronic, Philips. Jeffrey W. Moses: Consultant: Abiomed. Ziad A. Ali: Grant support and Consultant—St. Jude Medical. Richard A. Shlofmitz: Speaker—CSI. Akiko Maehara: Grant support—Boston Scientific, St. Jude Medical for research fellows; consultant—Boston Scientific, OCT Medical Imaging; speaker fee—St. Jude Medical.

Ethical approval The study complied with the Declaration of Helsinki. Ethics committees of the study sites approved the protocol.

Informed consent All patients signed written informed consent forms.

References

1. Kastrati A, Mehilli J, Pache J et al (2007) Analysis of 14 trials comparing sirolimus-eluting stents with bare-metal stents. *N Engl J Med* 356:1030–1039
2. Valgimigli M, Tebaldi M, Borghesi M et al (2014) Two-year outcomes after first- or second-generation drug-eluting or bare-metal stent implantation in all-comer patients undergoing percutaneous coronary intervention: a pre-specified analysis from the PRODIGY study (PROlonging Dual Antiplatelet Treatment After Grading stent-induced Intimal hyperplasia study). *JACC Cardiovasc Interv* 7:20–28
3. Giacoppo D, Gargiulo G, Aruta P, Capranzano P, Tamburino C, Capodanno D (2015) Treatment strategies for coronary in-stent restenosis: systematic review and hierarchical Bayesian network

- meta-analysis of 24 randomised trials and 4880 patients. *BMJ* 351:h5392
4. Kang SJ, Mintz GS, Akasaka T et al (2011) Optical coherence tomographic analysis of in-stent neoatherosclerosis after drug-eluting stent implantation. *Circulation* 123:2954–2963
 5. Nakazawa G, Otsuka F, Nakano M et al (2011) The pathology of neoatherosclerosis in human coronary implants bare-metal and drug-eluting stents. *J Am Coll Cardiol* 57:1314–1322
 6. Goto K, Zhao Z, Matsumura M et al (2015) Mechanisms and Patterns of Intravascular ultrasound in-stent restenosis among bare metal stents and first- and second-generation drug-eluting stents. *Am J Cardiol* 116:1351–1357
 7. Waksman R, Kitabata H, Prati F, Albertucci M, Mintz GS (2013) Intravascular ultrasound versus optical coherence tomography guidance. *J Am Coll Cardiol* 62:S32–S40
 8. Kyono H, Guagliumi G, Sirbu V et al (2010) Optical coherence tomography (OCT) strut-level analysis of drug-eluting stents (DES) in human coronary bifurcations. *EuroIntervention* 6:69–77
 9. Gonzalo N, Serruys PW, Garcia-Garcia HM et al (2009) Quantitative ex vivo and in vivo comparison of lumen dimensions measured by optical coherence tomography and intravascular ultrasound in human coronary arteries. *Rev Esp Cardiol* 62:615–624
 10. Tearney GJ, Regar E, Akasaka T et al (2012) Consensus standards for acquisition, measurement, and reporting of intravascular optical coherence tomography studies: a report from the international working group for intravascular optical coherence tomography standardization and validation. *J Am Coll Cardiol* 59:1058–1072
 11. Mehran R, Dangas G, Abizaid AS et al (1999) Angiographic patterns of in-stent restenosis: classification and implications for long-term outcome. *Circulation* 100:1872–1878
 12. Yabushita H, Bouma BE, Houser SL et al (2002) Characterization of human atherosclerosis by optical coherence tomography. *Circulation* 106:1640–1645
 13. Prati F, Guagliumi G, Mintz GS et al (2012) Expert's OCTR. Expert review document part 2: methodology, terminology and clinical applications of optical coherence tomography for the assessment of interventional procedures. *Eur Heart J* 33:2513–2520
 14. Barlis P, Dimopoulos K, Tanigawa J, Dzielicka E, Ferrante G, Del Furia F, Di Mario C (2010) Quantitative analysis of intracoronary optical coherence tomography measurements of stent strut apposition and tissue coverage. *Int J Cardiol* 141:151–156
 15. Radu MD, Raber L, Kalesan B et al (2014) Coronary evaginations are associated with positive vessel remodelling and are nearly absent following implantation of newer-generation drug-eluting stents: an optical coherence tomography and intravascular ultrasound study. *Eur Heart J* 35:795–807
 16. Inaba S, Mintz GS, Yun KH et al (2014) Mechanical complications of everolimus-eluting stents associated with adverse events: an intravascular ultrasound study. *EuroIntervention* 9:1301–1308
 17. Yonetsu T, Kim JS, Kato K et al (2012) Comparison of incidence and time course of neoatherosclerosis between bare metal stents and drug-eluting stents using optical coherence tomography. *Am J Cardiol* 110:933–939
 18. Yokoyama S, Takano M, Yamamoto M et al (2009) Extended follow-up by serial angioscopic observation for bare-metal stents in native coronary arteries: from healing response to atherosclerotic transformation of neointima. *Circulation Cardiovasc Interv* 2:205–212
 19. Otsuka F, Vorpahl M, Nakano M et al (2014) Pathology of second-generation everolimus-eluting stents versus first-generation sirolimus- and paclitaxel-eluting stents in humans. *Circulation* 129:211–223
 20. Lee SY, Hur SH, Lee SG et al (2015) Optical coherence tomographic observation of in-stent neoatherosclerosis in lesions with more than 50% neointimal area stenosis after second-generation drug-eluting stent implantation. *Circulation Cardiovasc Interv* 8:e001878
 21. Cook S, Ladich E, Nakazawa G et al (2009) Correlation of intravascular ultrasound findings with histopathological analysis of thrombus aspirates in patients with very late drug-eluting stent thrombosis. *Circulation* 120:391–399
 22. Chakravarty T, White AJ, Buch M et al (2010) Meta-analysis of incidence, clinical characteristics and implications of stent fracture. *J Am Coll Cardiol* 106:1075–1080
 23. Kuramitsu S, Hiromasa T, Enomoto S et al (2015) Incidence and clinical impact of stent fracture after PROMUS element platinum chromium everolimus-eluting stent implantation. *JACC Cardiovasc Interv* 8:1180–1188
 24. Kang SJ, Lee CW, Song H et al (2013) OCT analysis in patients with very late stent thrombosis. *JACC Cardiovasc Imaging* 6:695–703
 25. Otsuka F, Byrne RA, Yahagi K et al (2015) Neoatherosclerosis: overview of histopathologic findings and implications for intravascular imaging assessment. *Eur Heart J* 36:2147–2159
 26. Taniwaki M, Windecker S, Zaugg S et al (2015) The association between in-stent neoatherosclerosis and native coronary artery disease progression: a long-term angiographic and optical coherence tomography cohort study. *Eur Heart J* 36:2167–2176
 27. Alfonso F, Cuesta J, Bastante T, Aguilera MC, Benedicto A, Rivero F (2016) In-Stent Restenosis Caused by a Calcified Nodule: a Novel Pattern of Neoatherosclerosis. *Can J Cardiol* 32:830–e1
 28. Magalhaes MA, Minha S, Chen F et al (2014) Presentation and outcomes of coronary in-stent restenosis across 3-stent generations. *Circulation Cardiovasc Interv* 7:768–776